CrystEngComm

Accepted Manuscript

ROYAL SOCIETY OF CHEMISTRY

www.rsc.org/crystengcomm

Homo- and heteroepitaxial growth of Sn-doped β-Ga_2O_3 layers by MOVPE

D. Gogova[1,*], M. Schmidbauer[2], A. Kwasniewski[2]
[1] Central Lab of Solar Energy and New Energy Sources at the Bulg. Acad. Sci., Tzarigradsko shosee 72, Sofia, Bulgaria
[2] Leibniz Institute for Crystal Growth, Max-Born-Str. 2, 12 489 Berlin, Germany

Abstract
Layers of β-Ga_2O_3 in-situ doped with Sn were grown on Al_2O_3 (0001) and on native β-Ga_2O_3 (100) substrates by metal organic vapor phase epitaxy. Homoepitaxial growth of good-quality Sn-doped β-Ga_2O_3 layers with Rocking curve values comparable to that of Czochralski grown β-Ga_2O_3 substrates, was attained. Sn incorporation in a wide range of concentrations (from 10^{17} to 10^{19} cm^{-3}) was obtained without disturbing the crystallinity of the material grown. The interplay between deposition conditions, structural and electrical properties of the layers was studied. The Ga-vacancies-related defects and the residual from Ga-containing organic precursor carbon-related complexes have been revealed as acceptors compensating intentionally introduced Sn donors. The advantage of employment of the melt grown β-Ga_2O_3 crystals as homo-substrates for deposition of good-quality β-Ga_2O_3 layers is demonstrated. For the first time n-type homoepitaxial semiconducting β-Ga_2O_3 layers were attained by MOVPE. The good quality of the epilayers was elucidated through HR-XRD measurements and FWHM of the Rocking curve of the (100) peak of 43 arcsec was obtained, comparable to those of the Czochralski grown β-Ga_2O_3 substrates, and demonstrating similar dislocation densities for epilayers and substrates.

Novelty: For the first time n-type homoepitaxial semiconducting β-Ga_2O_3 layers were attained by MOVPE.

Introduction

Group III-sesquioxides has been discovered recently as a new class of wide-band-gap semiconductors. In the past polycrystalline highly doped In_2O_3:Sn(Ga) layers were employed as a transparent conductive material for transparent electrodes in "smart windows",[1,2] photo-voltaics,[1] large-area flat panel displays,[3] etc. Nowadays, the research is focusing on development of single-crystalline III-sesquioxides with low defect densities and semiconducting behavior to be used as active layers in electronic devices. The thermodynamically stable β-Ga_2O_3 phase is the most attractive representative of this class of materials due to its large band-gap (4.85 eV, which is the third largest band-gap among semiconductors) promising applications in short wavelength photonics and transparent electronics.[4] Moreover, it's high break-down field value (8 MV/cm), exceeding that of Si, GaAs, SiC, III-nitrides and some technologically relevant oxides, like ZnO, is very prospective for high power electronics. Also, Baliga's figure of merit for β-Ga_2O_3 is several times larger than that of 4H-SiC or GaN.[5] Furthermore, the unique properties of this material, combined with the availability of simple and low-cost, in comparison to GaN substrates[6], melt growth methods for mass production of bulk single crystals: Czochralski growth,[7] float zone growth,[8] and edge-defined film-fed growth (EFG)[9] have made β-Ga_2O_3 a strong candidate for next-generation power devices.

* Corresponding author E-mail address: dgogova@abv.bg

Nominally undoped films of β-Ga_2O_3 grown by metal organic vapor phase epitaxy (MOVPE) turned out to be insulating due to the large band-gap. To make them semiconducting, impurities such as Sn, Ge or Si have to be intentionally incorporated on Ga sites.[10] A theoretical study predicted that Sn is an efficient n-type dopant in β-Ga_2O_3.[10] We have chosen to study the behavior of Sn dopants since the Sn ionic radius is similar to that of Ga one, which should favour its incorporation. Moreover, in-situ Sn-doping of β-Ga_2O_3 material has been reported for bulk β-Ga_2O_3 grown by the floating zone method[11] and in MBE grown epitaxial β-Ga_2O_3 layers[12] only. X. Du *et al.* reported very recently n-type conductivity in MOVPE β-$Ga_{1-x}Sn_xO_3$ alloys (mixed oxides) with *x* from 1 to 10 at.% Sn.[13] Such very heavily doped oxides can be regarded as degenerate semiconductors.

Our main purpose is to develop MOVPE process for growth of Sn-doped β-Ga_2O_3 (β-Ga_2O_3:Sn) semiconducting layers. The interplay between growth regimes, structural and electrical properties of hetero- and homoepitaxial Ga-oxide layers will be discussed. The second aim is to check the Sn-doping potential in trimethylgallium (TMGa)-based MOVPE process. To the best of our knowledge such an investigation does not exist in the literature. For the first time n-type homoepitaxial β-Ga_2O_3:Sn semiconducting layers were attained by MOVPE.

Experimental

Substrate preparation

Bulk β-Ga_2O_3 single crystals were obtained from melt by the developed at IKZ Czochralski method using an iridium crucible and a dynamic, self-adjusting growth atmosphere to minimize the decomposition of Ga_2O_3 and oxidation of iridium crucible, as described in details elsewhere.[7] Semiconducting (nominally undoped) and semi-insulating (doped with Mg) crystals with diameter of 20-22 mm were grown along b-axis. From bulk single crystals epi-polished wafers were prepared. Both semiconducting and semi-insulating wafers were (100)-oriented.

Epitaxial growth of Sn-doped β-Ga_2O_3 thin films

Epitaxial thin films of β-Ga_2O_3 doped with Sn have been deposited on basal plane sapphire and on β-Ga_2O_3 (100) substrates with lateral sizes of 10x10 mm and 5x5 mm and with a thickness of 500 µm. The sapphire and Ga-oxide substrates undergo a thermal treatment in oxygen atmosphere at 950^{o}C for 1 h before the growth to obtain a damage-free surface with atomic steps.

MOVPE has been selected as a method of choice in this study due to the good crystalline material quality, it is able to achieve, combined with high growth rates applicable to electronic device fabrication on an industrial scale. Low-pressure MOVPE top-fed reactor with TMGa as a source of

gallium, and water vapors as a source of oxygen, were employed at the Leibniz Institute for Crystal Growth, Berlin, Germany. Tetraethyltin (TESn, $C_8H_{20}Sn$) has been taken as a tin precursor. The TESn bubbler temperature was kept at 5°C and that one of TMGa at -10°C and -12°C in different series of experiments to vary the concentration of Sn within some orders of magnitude. The reactor base pressure was changed from 500 to 5000 Pa. The flow rate of Ar carrier gas through the water bubbler was in the range 300-1000 sccm. The deposition temperature of the Sn-doped layers was fixed at: 775°C, 800°C, 825°C, and 850°C in different series of experiments. During the heating up and cooling down process the β-Ga_2O_3 (100) substrates and oxide thin films were kept in O_2-containing atmosphere to prevent any surface decomposition. The thickness of the β-Ga_2O_3:Sn layers was varied from 95 to 900 nm. A H_2O/Ga molar ratio from 187 to 2036 was employed. By adjustment of TMGa to Sn molar ratios from 77 to 32251, a series of β-Ga_2O_3:Sn layers with Sn concentration in the range from $1.6x10^{17}$ to $2.4x10^{19}$ cm^{-3} (determined by SIMS) was prepared.

First growth experiments have been performed on sapphire only in order to establish the growth window for deposition of β-Ga_2O_3:Sn crystalline layers. No any type of a buffer layer was employed. After optimization of the growth process parameters (temperature, base pressure, Ga/O ratio, Sn flux, etc.) and clarification of their impact on crystalline quality and growth rate, Al_2O_3 (0001) and β-Ga_2O_3 (100) substrates have been employed in one growth experiment to have a reliable basis for comparison of the homo- and heteroepitaxialy grown epilayers.

Some additional ex-situ annealing procedures for 1 h or 30 min at a temperature ranging from 850 to 1050°C in O_2-containing atmosphere were performed for the most of heteroepitaxially grown layers. Another group of samples was annealed in forming gas (5%H_2 in Ar) at 600 and 700°C to reach certain deviation from stoichiometry.

Characterization

Thin film surface morphology was studied by means of atomic force microscopy (AFM) and additionally by scanning electron microscopy (SEM) for confirmation of the AFM results. The Sn concentration was determined by secondary ion mass spectrometry (SIMS) using a standard, prepared by Sn ion implantation in a β-Ga_2O_3 bulk crystal.

The thickness of the doped Ga-oxide samples was determined by spectral ellipsometry and/or by glow discharge optical emission spectroscopy. The thickness values were independently confirmed by SIMS depth profile measurements. The crystalline quality of the layers, grown on sapphire, was investigated by x-ray diffraction (XRD), while high-resolution XRD experiments (HR-XRD) were

employed to record x-ray reciprocal space maps for the homoepitaxially grown layers. The bonding state and phase composition were studied by Raman spectroscopy. Hall effect measurements were performed for heteroepitaxially grown layers on sapphire and for homoepitaxial layers grown on semi-insulating (SI) β-Ga_2O_3 substrates.

The HRXRD experiments were carried out in a triple crystal set up (XRD Master HR, Seifert, CuKα radiation) in order to record X-ray reciprocal space maps with an angular resolution of about 11 arcsec for the homoepitaxially grown layers. Raman spectroscopy measurements were performed at room temperature in backscattering geometry by a Horiba Jobin Yvon spectrometer. For excitation, the 488 nm laser line of an Ar laser was employed. The carrier density and mobility in the semiconductor layers were determined by Hall effect measurements in van der Pauw configuration of the electrodes.

Results and discussion

Morphology and compositional study of the epitaxial layers

All thin films of β-Ga_2O_3:Sn, grown at temperatures from 775^{o}C to 850^{o}C at 500 Pa were homogeneous, highly transparent and exhibit smooth surface. A root mean square roughness ranging from 0.4 nm to 0.6 nm was evaluated on the basis of the AFM images (see Fig. 1). SEM studies have been also performed in order to have another independent assessment of the surface morphology. Most layers have been grown at oxygen-rich conditions to get less oxygen vacancies, highly transparent material and to decrease the incorporation of residual carbon. However, a small number of them were grown at close to Ga-rich conditions (characterized by formation of Ga droplets at the growing surface) to reach less Ga vacancies in the material that are known to be shallow donors with a negative ionization energy according to the theoretical study.[10] However, increasing the reactor base pressure leads to increased supersaturation and formation of some defects on the surface (Fig. 1b). The mechanism of their formation is still under investigation. First, the higher the base pressure in the reactor is the larger the ammount of incorporated Sn without β-Ga_2O_3 layer amorphisation is, which is importnt to get semiconducting single-crystalline samples (see the XRD and electrical properties sections below). Second, we need to grow at higher reactor base pressure in order to couple the growth windows of pure β-Ga_2O_3 and of indium, i.e. to be able to incorporate some In to explore its surfactant effect or for further growth of device heterostructures. Obviously, we have to make a compromise between the growth parameters values looking for the optimal combination of structural quality, surface morphology and electrical conductivity.

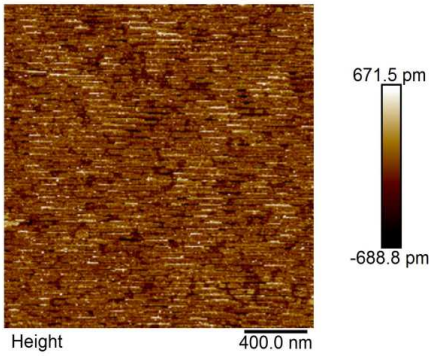

Fig. 1a AFM image typical of a Sn-doped layer grown at 800°C, 500 Pa, and miscut of the β-Ga_2O_3(100) substrate of 1.5°.

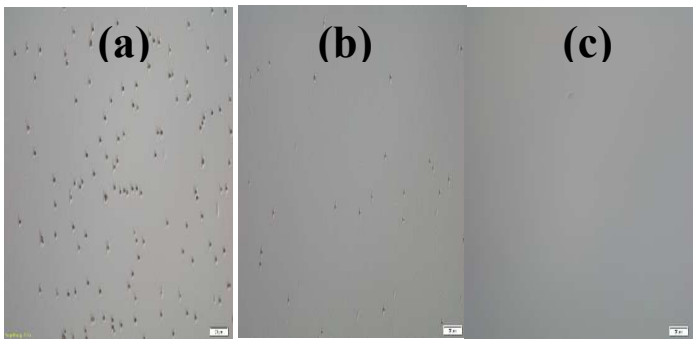

Fig. 1b Optical microscope study of the surface morphology of layers grown at 800°C but at different base pressures: (a) 2000 Pa; (b) 1000 Pa; (c) 500 Pa. The bar corresponds to 20 µm.

By adjustment of TMGa to TESn molar ratios from 215 to 32251, a series of β-Ga_2O_3:Sn layers with Sn concentration in the range from $1.2x10^{17}$ to $1x10^{19}$ cm^{-3} at 500 and 5000 Pa, determined by SIMS, was prepared. A high growth rate from 2.89 to 10.00 nm/min was achieved depending on the growth temperature and pressure mainly.

SIMS depth profiles (not shown here) demonstrate homogeneous Sn depth distribution through the whole thickness of the grown layers. Fig. 2 displays the concentration of the incorporated in the galium oxide layers Sn in dependence on the TESn molar flux. Obviously, the Sn concentration, estimated from SIMS, depends monotonically on the TESn flux in the semiconductor-relevant range of concentrations. The concentration of incorporated Sn for the rest of the samples grown was determined using the experimental points in Fig. 2 as a calibration curve.

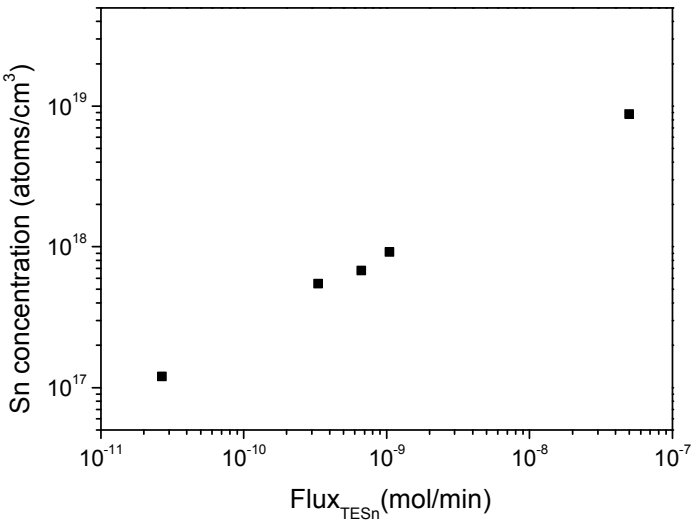

Fig. 2 Concentration of Sn incorporated in the β-Ga_2O_3:Sn layers, determined by SIMS in dependence on the TESn molar flux.

Structural properties study

X-ray investigations of the structure

XRD study of heteroepitaxially grown β-Ga_2O_3 layers

In Fig. 3 XRD diffraction spectra (2θ–ω–scans) of as-grown at 800°C and 5000 Pa, and annealed gallium oxide layer with a Sn-doping concentration of 1.60×10^{17} cm^{-3} are illustrated. The three sharp peaks at 2θ = 21.00°, 41.69°and 64.5° can be identified as the 00.3, 00.6 and 00.9 Bragg reflections of the c-plane sapphire, respectively. Additional peaks that appeared at 2θ = 18.9°, 37.8°, 58.7° and 80.7° are caused by the epitaxial layers and can be assigned to the -201, -402, -603 and -804 Bragg reflections of the monoclinic modification of Ga-oxide - the β-phase (see Ref. 14). No additional Brag peaks from the layer are observed providing that the Ga_2O_3 layer consists of the β-Ga_2O_3 phase only and that there exists a well-defined epitaxial relationship between the hexagonal (0001) Al_2O_3 substrate and the (-201)-oriented β-Ga_2O_3:Sn layers. However, the (-201)-oriented β-Ga_2O_3 layers on sapphire are epitaxially grown but not single-crystalline since there is an in-plane tilt between grains 120° rotated each to other due to the difference in crystal symmetry of substrate (hexagonal) and epilayer (monoclinic). Such grains were later on observed by TEM investigation.

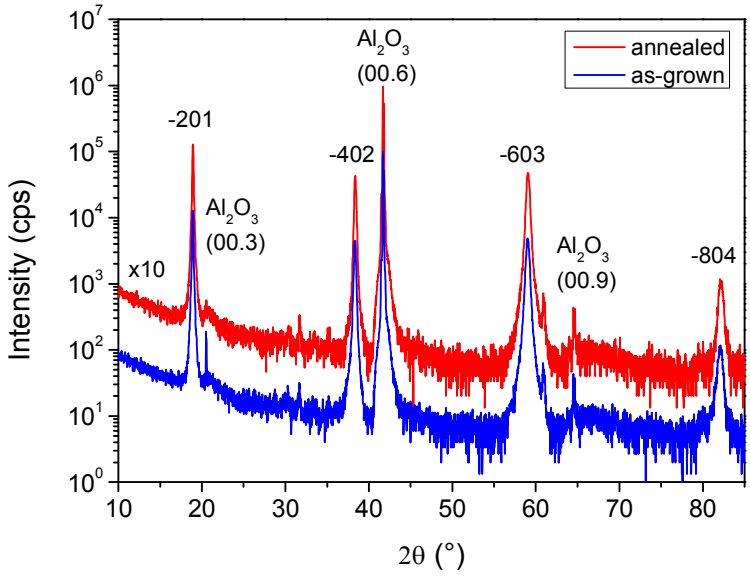

Fig. 3 XRD spectra typical of as-grown, at 800°C and 5000 Pa, and additionally annealed β-Ga_2O_3 layers with doping of $1.6x10^{17}cm^{-3}$ on sapphire substrates.

The as-grown sample (Fig. 3) exhibits a β-Ga_2O_3 film with very good structural properties and a lattice spacing (d_{-201} ≈ 4.691 Å) close to bulk value (d_{-201} = 4.690 Å). Annealing in oxygen-atmosphere does not change layer structural properties but a slightly reduced lattice parameter (d_{-201} = 4.689 Å) is observed.

Three typical XRD spectra (2θ–ω–scans) of β-Ga_2O_3:Sn layers grown at 800°C and 500 Pa on Al_2O_3 (0001) with different Sn doping are illustrated in Fig. 4a. Again, the -201, -402, -603 and -804 Bragg reflections of the monoclinic modification of gallium oxide are exclusively observed. However, it is striking that the width of the -603 Bragg reflections of the β-Ga_2O_3 layers is very large whereas the widths of the -402 and -804 Bragg reflections are quite small. This peculiarity, typical of the layers grown at 500 Pa, is not fully understood yet. We, however, suspect that a high density of stacking faults (SFs), which leads to a distinct vertical disorder in diffracting lattice planes, is the reason for this characteristic behavior.

The impact of Sn-doping on the structural quality of β-Ga_2O_3:Sn layers grown at 500 Pa is also depicted in Fig. 4a. For Sn-doping levels between $1.6x10^{17}$ to $0.9x10^{18}$ cm^{-3} pronounced β-Ga_2O_3 Bragg reflections can be observed – (curves *a* and *b*) proving that β-Ga_2O_3:Sn films are crystalline. On the other hand, the lack of β-Ga_2O_3 Bragg peaks indicates amorphization of the heteroepitaxially grown films (curve *c*) when the Sn-doping is $2.4x10^{18}cm^{-3}$ at a growth temperature of 825°C.

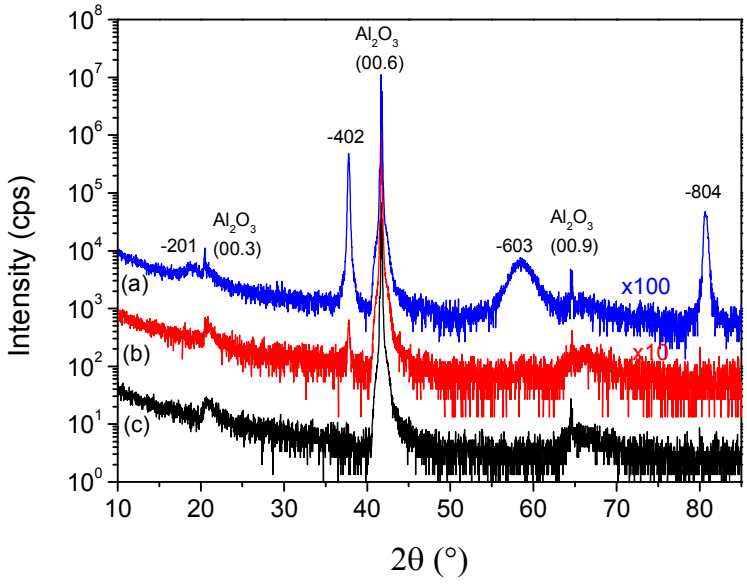

Fig. 4a $2\theta-\omega$ scans of β-Ga_2O_3:Sn films grown at equivalent conditions (800°C and 500 Pa) on Al_2O_3 (0001) with different Sn concentrations: (a) 1.6×10^{17} cm^{-3}, (b) 9×10^{17} cm^{-3} and (c) 2.4×10^{19} cm^{-3}

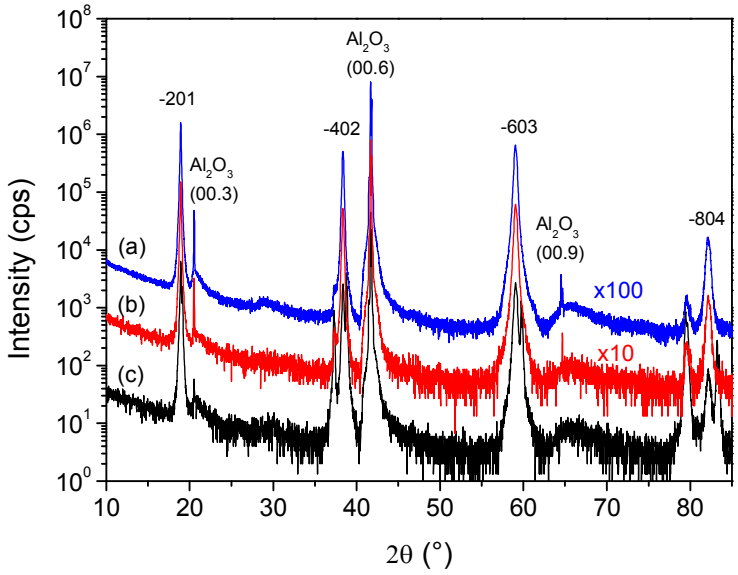

Fig. 4b $2\theta-\omega$ scans of β-Ga_2O_3:Sn layers grown at equivalent conditions (850°C and 5000 Pa) on Al_2O_3 (0001) with different Sn concentrations: (a) 5.6×10^{17} cm^{-3}, (b) 2.4×10^{18} cm^{-3} and (c) 8×10^{18} cm^{-3}

Fig. 4b demonstrates the impact of Sn-doping on the structural quality of β-Ga_2O_3:Sn layers at 5000 Pa for 3 different Sn concentrations. All spectra (from *a* to *c*) correspond to crystalline material. The XRD spectrum (c) is typical of a layer, grown with a largest TESn flux of $5x10^{-8}$ (mol/min). The sample is predominantly (-201)-oriented, .i.e., textured. The $2\theta-\omega$–scan (c) shows peaks that belong not only to the (-201) orientation of the β-phase of Ga_2O_3, i.e., there are some differently oriented grains in result of the high Sn doping concentration but the layers are still crystalline and not amorphisized as in the case of layers grown at 500 Pa. Obviously, in case of higher growth temperature and pressure the layer amorphization appears at a very high Sn-concentration – higher than $10^{19}cm^{-3}$, i.e. the lattice accumulates higher amount of dopants.

X-ray study of homoepitaxially grown β-Ga_2O_3 layers

The structural quality of the homoepitaxially grown layers was studied by X-ray reciprocal space mapping measurements. In Fig.5a an x-ray reciprocal space map of β-Ga_2O_3:Sn layer grown on (100) β-Ga_2O_3 substrate at 825^{o}C and 5000 Pa is illustrated.

(a) (b)

Fig. 5 X-ray reciprocal space map of a homoepitaxial β-Ga_2O_3:Sn layer grown at 825^{o}C and 5000 Pa on β-Ga_2O_3 (100) substrate in the vicinity of the 600 reciprocal lattice point (a) - Sn concentration – 1.2x10^{18} cm^{-3}) and (b) of a homoepitaxial β-Ga_2O_3:Sn layer grown at 850^{o}C and 5000 Pa on β-Ga_2O_3 (100) substrate in the vicinity of the 600 reciprocal lattice point. (Sn concentration - 9x10^{18} cm^{-3})

The reciprocal space map shown in Fig. 5 a exhibits two prominent peaks, which can be assigned as the (600) Bragg reflections of the β-Ga_2O_3 substrate (S) and the β-Ga_2O_3:Sn epilayer (L), respectively. The epilayer peak L is surrounded by weak thickness oscillations demonstrating

coherent crystal growth and smooth surface/interface. From the distance of the thickness oscillations we can determine the layer thickness to be 200 ± 5 nm. The relative distance between the two peaks S and L can be used to evaluate the vertical lattice spacing in the layer which is increased to that of the substrate by about $5x10^{-4}$. Fig. 5b depicts a similar RSM map of a layer grown at 850°C and with a Sn doping concentration of $9x10^{18}$ cm^{-3} . Here, only one strong peak (sitting on a low background level) can be observed. Obviously, the 600 Bragg reflections of substrate and epitaxial layer coincide proving that the vertical lattice parameter of both substrate and layer are identical, i.e. it demonstrates fully relaxed strain-free and coherent homoepitaxial growth (no difference in the lateral and vertical lattice parameters). To avoid any speculation on possible amorphisation of the homoepitaxially grown layer (substrate and layer peak coincide) the sample was additionally characterized by EBSD and the Kikuchi-like pattern obtained confirmed that the layer was single-crystalline and had the same orientation like the substrate (not shown here). Since this sample is relatively thick (750 nm) the corresponding thickness oscillations cannot be experimentally resolved in the RSM. The RSMs confirmed also that in contrast to heteroepitaxially grown on Al_2O_3 (0001) β-Ga_2O_3:Sn layers those grown on native substrates are single-crystalline and of good quality even at doping levels as high as $9x10^{18}cm^{-3}$.

The good crystalline quality of the epilayers, as high as that of the melt grown bulk substrate crystal was confirmed by HR-XRD Rocking curves measurements. The full width at half maximum (FWHM) of the (100) peak was estimated to be about 43 arcsec (Fig. 6) for a series of samples grown in the temperature range (800-850°C). This value is rather close to the typical of the employed Czochralski grown substrates: 25-35 arcsec, confirming good crystalline quality and similar dislocation densities for epilayers and substrates.

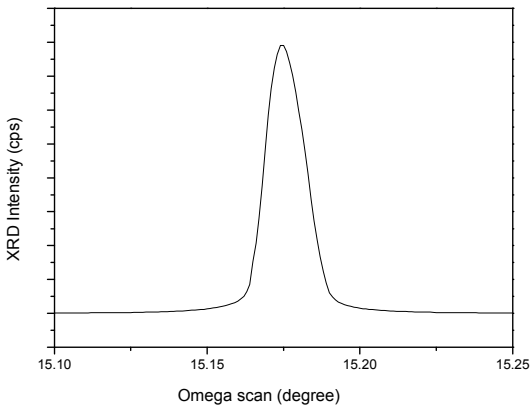

Fig. 6 A typical Rocking curve ⍰⍰scan of a β-Ga_2O_3:Sn layer

grown at 850°C and 5000 Pa.

Vibrational properties study

To further ensure the absence of foreign phases in the β-Ga_2O_3 crystals (substrate and layers) they were investigated by μ-Raman spectroscopy. A room temperature Raman spectrum typical of a homoepitaxial β-Ga_2O_3:Sn (100) layer (black curve) grown on a native substrate and a spectrum of the substrate (blue curve) in the lattice vibrations region, with a laser operating at 448 nm used for excitation, is depicted in Figure 7a. Several intense and narrow Raman modes can be observed. According to Dohy et al. [15] the modes at 114 cm^{-1}, 147 cm^{-1}, 169 cm^{-1} and 200 cm^{-1}, respectively are attributed to the vibration and translation of the doubly connected straight chains of GaO_6 edge shared octahedra running along the b-axis of the crystal. The Raman modes at 320 cm^{-1}, 349 cm^{-1}, 416 cm^{-1} and 475 cm^{-1}, respectively are connected to the deformation of the GaO_6 octahedra. The origin of the group of Raman modes located at 630 cm^{-1}, 657 cm^{-1} and 766 cm^{-1} represents the stretching and bending of GaO_4. The Raman peak positions of the layer and substrate coincide, i.e., we have a strain-free homoepitaxially grown β-Ga_2O_3 (100) layer. Here we have to mention that the Raman signal from the layer can not be separated from the stronger signal coming from the substrate since the penetration depth is larger than the layer thickness at the chosen excitation wavelength. Since only allowed β-Ga_2O_3 modes can be observed in the Raman measurements, there are no indicators for additional phases, i.e., no existence of additional: α, γ, δ or ε-Ga_2O_3 phase is observed) in the β-Ga_2O_3 samples.

By Raman spectroscopy in the local vibration modes region we observe very weak carbon-compound-related bands in the spectra of the epitaxial layers, grown at H_2O/Ga fluxes from 187 to 1000 (see black curve in Fig. 7 b), such as CO_2 at 1390 cm^{-1} and C-$H_{i=1-3}$ groups at about 2850 cm^{-1}. In the Raman spectra of layers grown at larger than 1000 H_2O to Ga flux ratios such carbon-related bands almost disappear due to the lower Ga molar fraction (respectively carbon) taking part in the chemical reaction. The information available in Handbooks on Raman and FTIR spectroscopy on that topic is rather limited, i.e., very broad zones are given for the vibrations of specific species, most likely for non-solid organic compounds (gases or liquids). For example, the C=C bands are located in the range 1500-1900 cm^{-1} and the C-H vibrations in the range 2800-3100 cm^{-1} (see Fig. 7b). At least for solids those vibrations should be better localized. The broader C-H bond of the substrate in Fig. 7b might be due to the back side contamination.

Reich and Thomsen[16] reported the position of the Raman band of graphite at 1582 cm^{-1}. In our spectra there is no any peak at that wave number, which means we do not have pure carbon incorporated in the MOVPE β-Ga_2O_3:Sn layers as a second phase.

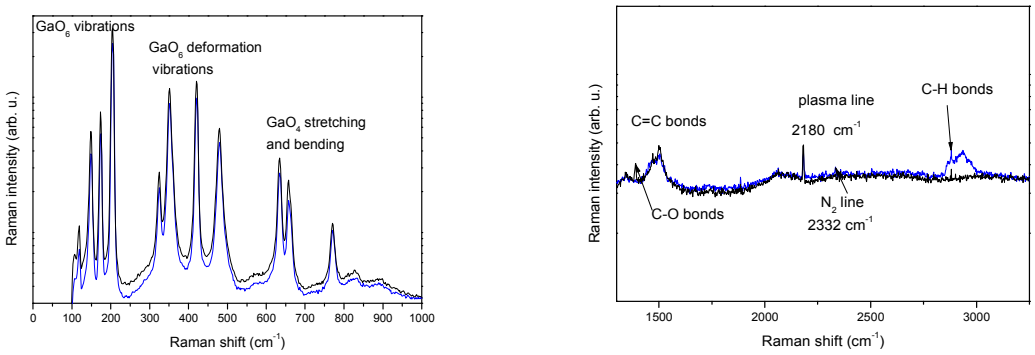

(a) (b)

Fig. 7 A typical RT Raman spectrum of a strain-free homoepitaxial β-Ga_2O_3 (100) layer (black curve) grown on a native substrate and a spectrum of the substrate (blue curve) in the lattice vibrations region - (a) and in the local vibration modes region - (b).

Electrical properties

Electrical properties study of heteroepitaxial β-Ga_2O_3 layers

Although SIMS shows that Sn is incorporated in the layers in the semiconducting range of concentrations, the Hall effect measurements of heteroepitaxial β-Ga_2O_3:Sn layers performed at RT demonstrate that the resulting material grown on sapphire is not electrically conductive.

Dopants must occupy the correct substitutional lattice position to become electrically active donors or acceptors. Heating, or thermal activation is the principal process used to move impurities into their substitutional sites. In an attempt to electrically activate the Sn-species, the epitaxial layers were annealed in O_2 at temperatures from 800 to 1050°C for 1 h/30min. However, neither one type of annealing (oxidizing or reducing) has changed the resistivity of the samples, i.e. they remained semi-insulating.

Based on DFT, Varley et al.[10] calculated the formation energies and charge state transition levels for oxygen vacancies and donor impurities in β-Ga_2O_3. They found that Si, Ge, Sn, and H behave as shallow donors. Why is the electrical activity of the Sn species so poor and why are we unable to observe free electrons? Similar effect we have observed in the case of doping with Si[17]. Here, we have to take into account that the mismatch, in crystal symmetry, lattice constants and thermal

expansion coefficients between β-Ga_2O_3 epitaxial layers and the hexagonal sapphire substrates, gives rise to a high density of defects (mainly SFs, as observed by HR-TEM[17]) and strain, limiting, e.g., the electron mobility and doping efficiency. Thus, the reason for the high resistivity of our β-Ga_2O_3:Sn films could come from the compensation of the Sn-donors by stacking faults.

Moreover, theoretical studies have shown that the formation of Ga-vacancies at oxygen-rich conditions, like in the present study, may have even a negative formation energy. To highlight these aspects some more investigations have been performed. The first one of them was SIMS measurements of the residual carbon concentration in our β-Ga_2O_3:Sn layers. However, since carbon is a common contaminant the total carbon concentration in the layers was not reliably determined by SIMS.

It is known that C has ambipolar behavior in the case of exhaustively studied GaN[18]. We suppose similar behavior of carbon to exist in gallium oxide also, and C on O-site in our case plays the role of an acceptor. Obviously, we have compensation of the Si- and Sn-donors by C (or C-related complexes), which is a residual from the metalorganic precursors. An indirect proof that carbon is an acceptor in β-Ga_2O_3 could be the effect of charging of β-Ga_2O_3:C standard during the SIMS measurements, i.e., the initially semiconducting β-Ga_2O_3 crystal has turned into semi-insulating one after implantation of carbon ions.

It is not known so far whether some of the carbon occupies gallium sites acting as a donor, interstitial sites creating states in the midgap region, and/or is tied up in the dislocations or SFs in the layers where it is not electrically active. It is even possible C to form some complexes with Sn. Secondly, the doped samples have been studied by positron annihilation life-time spectroscopy (PALS) (details have been reported additionally[19]). In general, by this method it has been shown that all doped with IV-group species layers, grown at oxygen-rich conditions, like in the present study, have considerable amount of Ga vacancies (acceptors) - higher than 10^{17} cm^{-3} - that contributes to the electrical compensation of the intentionally in-situ introduced donors.

Electrical properties study of homoepitaxial β-Ga_2O_3 layers

However, Hall effect measurements carried out on highly doped (up to $8x10^{18}$ cm^{-3}) β-Ga_2O_3 (100) grown on SI native substrates showed that they were conductive. By Hall measurements, the room temperature free-electron concentration and mobility were determined to be N=-$7.1x10^{17}$ cm^{-3} and μ=13.7 cm^2V^{-1} s^{-1}, respectively (see Table 1). Conductivity of 1 S cm^{-1}, electron mobility: 0.44 cm^2V^{-1} s^{-1} for carrier density of $1.4x10^{19}$ cm^{-3} was reported by Hosono et al. for pulsed laser deposited (carbon-free deposition) β-Ga_2O_3 layers on quartz.[20] Better mobility of 40 cm^2V^{-1} s^{-1} at

high 10^{18} cm^{-3} doping and 100 cm^2V^{-1} s^{-1} at 10^{17} cm^{-3}, respectively, is attained by ozone MBE (carbon-free) homoepitaxially grown layers on EFG β-Ga_2O_3 substrates (010)-oriented only.[9] The growth rate,[9] and most likely electron mobility in (010)-direction is larger than for the (100)-one. Low-temperature electrical measurements, however, did not show a typical for semiconductor temperature behavior, i.e., our material is compensated.

Table 1 illustrates the RT Hall effect free-electron concentration and mobility results as well as the Sn dopant concentration determined by SIMS for 3 samples with different doping concentration. Obviously, there is a difference in the donor concentrations of at least one order of magnitude, i.e., not all physically incorporated Sn donors are electrically active at room temperature as it is expected. As we discussed above the reasons for compensation of our TMGa-based MOVPE β-Ga_2O_3 are Ga-vacancies, carbon-related defects and SFs. Varley has calculated very recently by DFT that C-H groups are acceptors in β-Ga_2O_3 and compensate the intentionally introduced donors.[21] We have observed in our TMGa-based gallium oxides C-H related bands by Raman spectroscopy, i.e. C-H exist in the Sn-doped layers and should contribute to the electrical compensation we observe by electrical measurements.

Sample number	Room temperature Hall effect free-electron concentration (cm^{-3})	RT Hall effect mobility μ (cm^2V^{-1} s^{-1})	SIMS Sn concentration (cm^{-3})
A	$6x10^{17}$	10	$8x10^{18}$
B	$7.1x10^{17}$	13.7	$3.6x10^{18}$
C	Not measurable	Not measurable	$5x10^{17}$

Table 1: Room temperature Hall effect data and SIMS determined Sn concentration for 3 samples with different doping.

Further improvement of the electron mobility and more precise control over n-type doping of MOVPE β-Ga_2O_3 will be achieved by employment of a less carbon-containing Ga-precursor (commercially available or specially designed) and growth close to Ga-rich conditions (to be reported additionally). Concerning the electrical quality of the layers we have reached its worldwide maximal performance, that is limited by the properties of the employed TMGa-precursor. In case of oxides growth due to the much lower growth temperature compared to those

of GaN, deposited by means of the same TMGa precursor at 1100°C (about 300°C higher temperature), the concentration of incorporated carbon and carbon-related defects is much higher. In summary, TMGa is not the best precursor for MOVPE growth of β-Ga_2O_3 since the TMGa-decomposition reaction and its products limit the initially high doping potential of Sn (as theoretically calculated). Nevertheless these obstacles, our TMGa-based material is of good crystalline quality, proved by HR-XRD, although of relatively high concentration of point defects and the existence of some surface defects in layers grown at high reactor base pressure.

MOVPE is an industry-relevant technique due to its high growth rate, good homogeneity on large areas and cost-effectiveness. However, MBE is an ultra-high vacuum technique for growth of state-of-the–art single-crystalline semiconducting or dielectric layers. These advantages are valid for the MBE and MOVPE growth of Sn-doped β-Ga_2O_3 too. So, we do not need to compete one very expensive and focused mainly on scientific problems growth technique with the other one that is relevant for device fabrication on industrial scale. MBE of Sn-doped β-Ga_2O_3 is a carbon-free method in comparison to the MOVPE one. Therefore, the effect of compensation caused by the C-H complexes does not exist in the case of MBE growth. Our purpose was to develop an industry-relevant process. Employment of an inorganic (carbon-free) VPE precursor can be even more advantages than the used in the present study largly applicable in III-Vs or III-Ns compounds TMGa precurssor. However, with this paper we pave the way to successful employment of the MOVPE technique for growth of semiconducting Ga-oxide layers. Further improvements in terms of better process control and employment of more advantages precursors in under way.

Conclusions

Monoclinic β-phase Ga_2O_3 layers doped with Sn have been heteroepitaxially grown on Al_2O_3 (0001) substrates by low-pressure MOVPE. The β-Ga_2O_3:Sn films are (-201)-oriented and exhibit an epitaxial relationship with the hexagonal substrate. SIMS measurements showed that Sn may be incorporated in the semiconducting range of concentrations. A high growth rate (up to 10 nm/min) and carrier concentration over the range of 10^{17}–$10^{18}$$cm^{-3}$ were achieved. The role of Ga-vacancies-related defects and intrinsically contained carbon-related complexes as acceptors in β-Ga_2O_3:Sn has been indicated. Homoepitaxial growth of good-quality *n*-type doped β-Ga_2O_3:Sn semiconducting single-crystalline layers is demonstrated for the first time by MOVPE. The good quality of the epilayers was elucidated through HR-XRD measurements and FWHM of the Rocking curve of the (100) peak of 43 arcsec was obtained, comparable to those of the Czochralski grown bulk β-Ga_2O_3 substrates, and demonstrating similar dislocation densities for epilayers and substrates. Achievement of more precise control over n-type doping will be realized by employment of a new less-carbon containing organic or inorganic Ga-precursor and growth close to metal-rich conditions.

Acknowledgements: We thank Dr. Z. Galazka for providing the β-Ga_2O_3 substrates, Dr. G. Wagner for the financial support, Dr. K. Irmscher for the electrical measurements and Dr. M. Albrecht for the fruitful discussion.

References

1 C. G. Granqvist, *Nature Materials,* 2006**, 5**, 89-90.

2 D. Gogova, L.-K. Thomas and B. Camin, *Thin Solid Films,* 2009, **517** (11), 3326-3331.

3 U. Betz, M. Kharrazi Olsson, J. Marthy, M.F. Escolá, F. Atamny, *Surf. Coatings Techn*., 2006, **200**, 5751–5759.

4 J. Wager, *Science* 2003, **300** (5623) 1245-1246.

5 B. Jayant Baliga, *IEEE Electron Device Lett*., 1989, **10**, 455-457.

6 D. Gogova, P. P. Petrov, M. Buegler, M. R. Wagner, C. Nenstiel, G. Callsen, M. Schmidbauer, R. Kucharski, M. Zajac, R. Dwilinski, M. R. Phillips, A. Hoffmann, and R. Fornari, *J. Appl. Phys*., 2013, **113**, 203513.

7 Z. Galazka, R. Uecker, K. Irmscher, M. Albrecht, D. Klimm, M. Pietsch, M. Brützsam, R. Bertram, S. Ganschow, and R. Fornari, *Cryst. Res. Technol*., 2010, **45**, 1229- 1236.

8 E.G. Villora, K. Shimamura, Y. Yoshikawa, K. Aoki, N. Ichinose, *J. Cryst. Growth*, 2004, **270**, 420-424.

9 Kohei Sasaki, Akito Kuramata, Takekazu Masui, Encarnacion G. Vıllora, Kiyoshi Shimamura, and Shigenobu Yamakoshi, *Appl. Phys. Express,* 2012, **5**, 035502; www.tamura-ss.co.jp

10 J. B. Varley, J. R. Weber, A. Janotti, and C. G. Van de Walle, *Appl. Phys. Lett*., 2010, **97**, 142106.

11 N. Suzuki, S. Ohira, M. Tanaka, T. Sugawara, K. Nakajima, T. Shishido, *phys. stat. sol. (c)*, 2007, ***4*** (7) 2310–2313 .

12 Masataka Higashiwaki, Kohei Sasaki, Akito Kuramata, Takekazu Masui, and Shigenobu Yamakoshi, *Appl. Phys. Lett.,* 2012, **100**, 013504 .

13 L. Binet, and D. Gourier, *J. Phys. Chem. Solids*, 1998, **59**(8), 1241-1249.

14 *Joint Committee on Powder Diffraction Standards* (JCPDS, PDF No. 43043-1012 and 041-1103).

15 D. Dohy, G. Lucazeau, and A. Revcolevschi, *J. Solid State Chem*. 1982, **45(2)**, 180-192.

16 Stephanie Reich and Christian Thomsen, *Phil. Trans. R. Soc. Lond. A*, 2004, ***362***, 2271–2288.

17 D. Gogova, G. Wagner, M. Baldini, M. Schmidbauer, K. Irmscher, R. Schewski, Z. Galazka, M. Albrecht, R. Fornari, *J. Cryst. Growth,* 2014, **401**, 665-669.

18 C. H. Seager, A. F. Wright, J. Yu and W. Götz, *J. Appl. Phys*., 2002, **92 (11)**, 6553-6560.

19 E. Korhonen, F. Tuomisto, D. Gogova, G. Wagner, M. Baldini, Z. Galazka, R. Schewski, and M. Albrecht, *Appl. Phys. Lett*., 2015, **106**, 242103.

20 Masahiro Orita, Hiromichi Ohta, Masahiro Hirano, Hideo Hosono, *Appl. Phys. Lett*., 2000, **77**, 4166.

21 J. B. Varley, *private communication*.